

Optical Engineering

OpticalEngineering.SPIEDigitalLibrary.org

Design of a dynamic biofilm imaging cell for white-light interferometric microscopy

Curtis Larimer
Michelle Brann
Jonathan D. Suter
R. Shane Addleman

SPIE.

Curtis Larimer, Michelle Brann, Jonathan D. Suter, R. Shane Addleman, "Design of a dynamic biofilm imaging cell for white-light interferometric microscopy," *Opt. Eng.* **56**(11), 111708 (2017), doi: 10.1117/1.OE.56.11.111708.

Design of a dynamic biofilm imaging cell for white-light interferometric microscopy

Curtis Larimer, Michelle Brann, Jonathan D. Suter, and R. Shane Addleman*

Pacific Northwest National Laboratory, Signatures Science and Technology Division, Richland, Washington, United States

Abstract. In microbiology research, there is a strong need for next-generation imaging and sensing instrumentation that will enable minimally invasive and label-free investigation of soft, hydrated structures, such as bacterial biofilms. White-light interferometry (WLI) can provide high-resolution images of surface topology without the use of fluorescent labels but is not typically used to image biofilms because there is insufficient refractive index contrast to induce reflection from the biofilm's interface. The soft structure and water-like bulk properties of hydrated biofilms make them difficult to characterize *in situ*, especially in a nondestructive manner. We build on our prior description of static biofilm imaging and describe the design of a dynamic growth flow cell that enables monitoring of the thickness and topology of live biofilms over time using a WLI microscope. The microfluidic system is designed to grow biofilms in dynamic conditions and to create a reflective interface on the surface while minimizing disruption of fragile structures. The imaging cell was also designed to accommodate limitations imposed by the depth of focus of the microscope's objective lens. Example images of live biofilm samples are shown to illustrate the ability of the flow cell and WLI instrument to (1) support bacterial growth and biofilm development, (2) image biofilm structure that reflects growth in flow conditions, and (3) monitor biofilm development over time nondestructively. In future work, the apparatus described here will enable surface metrology measurements (roughness, surface area, etc.) of biofilms and may be used to observe changes in biofilm structure in response to changes in environmental conditions (e.g., flow velocity, availability of nutrients, and presence of biocides). This development will open opportunities for the use of WLI in bioimaging. © The Authors. Published by SPIE under a Creative Commons Attribution 3.0 Unported License. Distribution or reproduction of this work in whole or in part requires full attribution of the original publication, including its DOI. [DOI: [10.1117/1.OE.56.11.111708](https://doi.org/10.1117/1.OE.56.11.111708)]

Keywords: white-light interferometry; biofilm; bacteria; nondestructive; imaging; flow cell; topology; roughness.

Paper 170034SSP received Jan. 5, 2017; accepted for publication Apr. 21, 2017; published online May 10, 2017.

1 Introduction

Biofilms are communities of microbes that attach to surfaces.¹⁻³ They are ubiquitous in the environment and can have beneficial or deleterious effects on the host structure or organism. Dental plaque is an example of a biofilm that forms in the human body and may cause tooth decay without proper hygiene.⁴ On the other hand, a biofilm forming at the influent of a sand drinking water filter—the so-called “schmutzdecke”—contributes to removal of harmful bacteria and viruses despite the fact that it may be composed of a natural mixture of bacteria, fungi, protozoa, algae, and even insect larva.⁵ A characteristic of biofilms is the formation of a protective layer of excreted organic substances known as the extracellular polymeric substance (EPS). The EPS serves to ensure continuous hydration of a biofilm, aids adhesion to surfaces, and often increases the ability to withstand environmental fluxes and treatment with antibiotics or other antiseptic chemicals.⁶

The EPS layer influences the three-dimensional (3-D) architecture of biofilms, and this structure, in turn, has been shown to influence the severity or harmfulness of the biofilm on the host surface.⁷ As such, greater understanding of biofilm structure and its role in function may prove valuable in the fight against diseases that are either caused by or exacerbated by the formation of biofilms. It is

particularly important to study the early stages of biofilm formation because even a small level of bacterial colonization on a surface can lead to a serious infection on, for example, an implanted medical device. Biofilms are associated with a majority of chronic infections, where they are also increasingly resistant to traditional treatment methods, such as antibiotics.^{8,9}

Studying biofilms in their natural environments is challenging, and nondestructive experimental assay methods are needed.¹⁰ It is often desirable to study a biofilm without significantly impacting its normal structure and function because many important biological questions can only be answered by observing a biofilm's transition as a result of an external perturbation. For example, it may be important to identify the location and function of bacterial cells that persist after treatment with antibiotics.¹¹ These cells exhibit enhanced antibiotic resistance and can remain on a surface and repopulate a biofilm even after extended efforts to remove them. In a mature biofilm, cells can detach and spread biofilm infection to new locations. Figure 1 shows the process for biofilm formation and the mechanism for resistance to treatment.

Optical imaging is a preferred method for nondestructive observation of biofilms. Simple observation with bright-field microscopy can resolve cells and microscopic features. Confocal and fluorescent modalities build on bright-field microscopy with improved resolution, 3-D sectioning, and observation of fluorescent labels. However, each imaging technique shares a common limitation: high resolution

*Address all correspondence to: R. Shane Addleman, E-mail: Raymond.Addleman@pnnl.gov

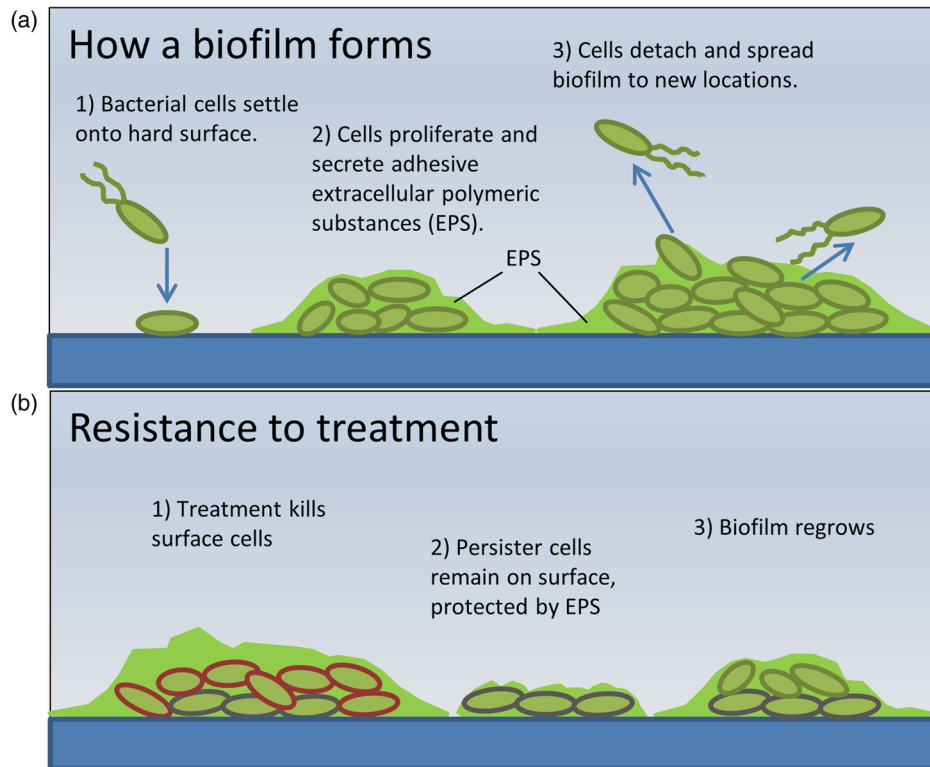


Fig. 1 (a) An illustration of the biofilm development process. Biofilms attach to a surface through excretion of EPS. They can then spread and release from surfaces to colonize new areas. (b) Resistance to treatment is mediated by EPS and by the existence of persister cells on the surface, which can repopulate a biofilm.

and high magnification necessarily limit field of view. Biofilms are spatially heterogeneous, so looking at a narrow field of view may give an incomplete picture of the biofilm's development and may, for example, miss the presence of remnant cells and other biomolecules. Remnant cells may enter a slowed metabolic state (i.e., persister cells), but, even if the cells are dead and merely adherent, they could hasten repopulation of a biofilm even if they are sparsely distributed. Likewise, imaging a large field of view results in poor resolution such that cells and EPS structures cannot be resolved. High-resolution electron microscopy techniques suffer from this limitation, and they typically require destructive sample preparation and exposure to high vacuum. Figure 2 shows a comparison of 3-D imaging techniques that have been applied to biofilms. Atomic force microscopy can provide very fine axial and lateral resolution but requires contact with the sample, which may be disruptive. Optical coherence tomography employs infrared light and has limited resolution as a result. Interferometric imaging [i.e., white-light interferometry (WLI)] is unique in its combination of high axial resolution and large field of view.

WLI offers unique capabilities for biofilm imaging. It is a noncontact, nondestructive optical technique that takes multiple bright-field optical images through a user-determined vertical range and uses interference in the images to recreate a 3-D topological map of the surface of the sample being imaged. In WLI, a broad spectrum light source with low coherence, such as a light-emitting diode (LED), is used to illuminate a sample. Light reflected from the sample is recombined with light reflected from a flat reference mirror to create an interference pattern on a camera sensor. The

short coherence length of the light means that interference only occurs over a narrow range when the sample is the same distance as the reference mirror. WLI gained its name from this phenomenon, although, in practice, light of any color may be used as long as it has a short coherence length. Until recently, the application of this technique in microbiology was limited due to the challenges of imaging in liquid media. A biofilm is largely composed of water and typically has a refractive index that is substantially similar to the bulk

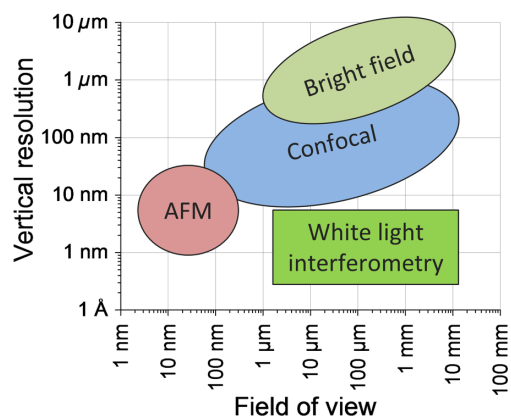


Fig. 2 Comparison of imaging modalities used to collect 3-D topographical information from biofilms. Typically higher resolution necessarily limits the field of view. The axial resolution of interferometric imaging is independent of magnification, so high-resolution imaging is possible even with a large field of view. This is valuable for imaging biofilms, which are spatially heterogeneous.

liquid in which it is grown.^{12,13} In short, the biofilm surface is not reflective, so it cannot be imaged using WLI, which requires reflection of light from the surface of interest. In some cases, living cells have been imaged through observation of subtle changes in the optical path length (OPL) of light reflected from a reflective substrate on which the cells are supported.^{14–16} With high axial resolution and a large field of view, WLI is well-suited to investigate the structure and topology of bacterial biofilms.

We recently reported a method for biofilm imaging with WLI that employs a small volume of air to create a reflective interface at the surface of a biofilm.¹⁷ The technique uses a fine needle to insert a microbubble between a glass coverslip and the surface of a biofilm. Bubbles are usually deleterious to biofilm studies in flow cells, and many strategies have been devised to remove them.¹⁸ However, in this case, the bubble provides a key advantage—it creates a highly reflective interface at the surface of the biofilm that is suitable for a reflection imaging technique, such as WLI. The method was previously demonstrated on biofilms grown under static conditions in petri dishes. In this work, the design of a flow cell suitable for WLI imaging is presented. Flow cells are commonly used for microscopy of biofilms as it is desirable to grow biofilm samples under dynamic conditions that more closely approximate conditions seen in nature.¹⁹ They are typically designed with influent and effluent channels leading to and from an imaging chamber. Imaging in flow cells is desirable because the dynamic flow conditions mean the biofilm's growth can be sustained for longer periods of time with a steady supply of nutrient media, and the system is amenable to the introduction of perturbations, chemicals, and therapies through the flow stream. Herein, we describe a flow cell that was designed to enable detailed imaging of biofilm structure as grown in dynamic and well-controlled conditions.

2 Methods and Materials

2.1 Flow Cell Assembly

A flow cell for WLI imaging of biofilms was designed with 3-D modeling software (Sketchup). The enclosure for the growth chamber was 3-D printed (Flashforge Dreamer) from acrylonitrile butadiene styrene via a polymer extrusion method. The enclosure was designed to support a substrate and viewing window parallel to one another with influent and effluent liquid channels on opposite ends. Thin glass coverslips (No. 2, 25 × 50 mm) were used for the viewing window and substrate (Ted Pella). A needle (31 G) was used to deliver liquid to the space between the viewing window and the substrate. Silicone adhesive was used to seal liquid between the two parallel windows. Silicone tubing was used to pump liquid media from a 1-L reservoir to the inlet of the flow cell. Similarly, effluent liquid was pumped to a waste container via silicone tubing. A peristaltic pump (Ismatec REGLO) was used to move liquid through influent and effluent tubing. A wye connection was placed in the tubing just before the inlet with a septum on one branch. The flow cell design will be described in further detail below.

2.2 Biofilm Culturing

A culture of *Pseudomonas fluorescens* (ATCC 13525) was grown overnight in liquid nutrient broth (BD Biosciences) on

a rotating platform at room temperature. *P. fluorescens* is a common gram-negative bacterium that is found in soil and water. A 100- μ L aliquot of the bacteria was used to inoculate a 1-L bottle of sterile nutrient broth, which served as the reservoir for the flow cell system. Bacteria colonized the imaging chamber naturally, and biofilm was allowed to grow unimpeded for 24 h before imaging. The flow rate was \sim 300 mL/day—media was not circulated.

2.3 Interferometric Imaging of Biofilm Growth in Flow Cell

Biofilms were imaged with a white-light interferometric microscope (Bruker Contour Elite GT-I). A 2.5 \times interferometric objective lens was used; 0.55 \times and 2 \times field of view lenses were also utilized. The flow cell was fixed on the microscope's translating stage, and flow was temporarily interrupted during measurement. While the flow cell enables growth of biofilms in dynamic conditions, it is necessary to temporarily pause the flow for imaging because WLI is highly sensitive to sample movement. An air bubble (\sim 300 μ L) was introduced into the imaging chamber of the flow cell through a septum attached to the wye connection just before the inlet. Standard procedures were used to find the focus and level the viewing window of the flow cell. Then, the objective was lowered and scanned through a range designed to capture interference fringes from the lower surface of the viewing window and the biofilm without collecting data from the upper surface of the viewing window or any other surfaces. Raw frame data were saved and analyzed separately from the 3-D profile generated by the instrument software. Bruker's Vision64 software was used for limited data processing and controlling the instrument. Data were also analyzed in both MATLAB[®] and open source 3-D data visualization software (Gwyddion). At the conclusion of data collection, the flow of liquid media was resumed and the air bubble in the imaging chamber was removed through the effluent channel.

3 Results and Discussion

3.1 Flow Cell Design

Prior use of WLI to image biofilms was done by placing a clean coverslip over a biofilm and inserting an air bubble under it.¹⁷ Light was transmitted through the top viewing glass, but, because it did not have any surface attached bacteria, light could pass through to the biofilm growing on the substrate. At the end of the imaging process, the coverslip was removed, cleaned, and dried before being used for subsequent images. Building an enclosed flow cell offers the advantages of greater control over growth conditions and less impact on the fragile biofilm structures during imaging. However, a significant challenge of using a fixed viewing window that remains in contact with the inoculated liquid is the inevitable accumulation of biofilm on the viewing window. The flow cell was, therefore, designed such that the top viewing window also served as the growth surface for biofilm. For imaging, light passed through the viewing window and the biofilm before being reflected from the lower surface of the biofilm. Compared to the static imaging method, this significantly simplifies calculation of biofilm thickness and reduces the scanning range needed, which also reduces the time needed for measurement. A drawback is that light must

pass through the biofilm twice, which limits the technique to biofilms that are partially transparent. It is straightforward to observe the smooth lower edge of the viewing window and measure the distance to the surface of the biofilm. Since WLI is usually performed in air, a scaling factor equal to the refractive index of the medium (i.e., the biofilm) is needed to calculate the thickness.

Figure 3 is a 3-D model of the flow cell used to image biofilms. Its salient details are (1) the large area viewing window, (2) the inlet and outlet tubing that supply nutrient media, and (3) the enclosure that supports the viewing window and maintains a fully enclosed environment for biofilm growth. Latex sheets (McMaster-Carr) of the desired thickness (300 μm) were used to create a gasket, and silicone glue (GE 280) secured the two layers together to create a watertight seal. Tube coupling fittings and sockets (McMaster-Carr) allowed for access and connection to the silicone rubber tubing (McMaster-Carr) that connected the imaging cell to the peristaltic pump. The tubing connected the flow cell to the reservoir of nutrient broth and the waste reservoir.

Figure 4 gives a more detailed view of the biofilm growth chamber. The viewing window and substrate are parallel to one another and form a thin volume for biofilm growth. This chamber is thick enough ($\sim 300 \mu\text{m}$) to support the development of biofilm structures that are much larger than the individual bacteria (1 to 10 μm). However, the space between the viewing window and the substrate was limited to ensure that small bubbles that enter the chamber will be pressed against the biofilm surface. Figure 4 shows that chamber is full of liquid, and biofilm accumulates on the top and bottom surfaces of the chamber when the flow cell is in growth mode. The only change necessary for imaging is the introduction of a bubble, which displaces liquid broth but cannot displace the biofilm, which is more firmly attached to the surface. For initial experiments, air was used to create the bubble, though other gases could be used if anaerobic conditions are desired. Overall, the flow cell enables imaging of biofilms grown in dynamic conditions. The large viewing window makes it possible to observe large-scale biofilm features and heterogeneity in the way that the biofilm forms. The flow cell makes it easy to introduce perturbations to the environment and observe resultant changes in biofilm structure. For example, in future experiments, it will be possible to observe the effects of antibiotics and other antibiofilm therapies by

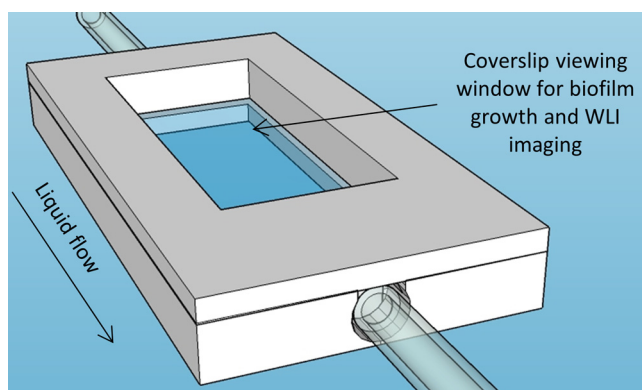


Fig. 3 3-D model of a flow cell used to grow and image biofilms. The viewing window serves as a support for biofilm growth and enables interferometric imaging. The viewing window is 25 \times 50 mm.

introducing the drugs into the liquid stream. This offers a controlled way to study biofilm persistence.

3.2 Selection of Imaging Window

An important consideration when imaging biofilms in a closed flow system is the selection of the viewing window. Glass coverslips are typically placed over objects for viewing with an optical microscope where their main function is to keep the sample flat and to prevent contact between the immersion liquid (typically oil or water) and the sample. Coverslips are not typically used with WLI imaging because there is no immersion liquid and because the smooth glass would obscure the texture of the underlying sample. For biofilm imaging with WLI, the coverslip is integrated into a flow cell and serves to contain the liquid media that supports bacterial growth. Bacterial adhesion is nonspecific and forms on all interior surfaces of the flow cell, including the bottom of the coverslip. The coverslip serves as the growth surface for biofilm that is to be imaged and as a viewing window. As with any interferometric imaging through transmissive media, it is important that the coverglass is transparent and smooth. The thickness of coverslip glass is a limiting factor when imaging biofilms. Light transmitted through the higher index coverslip glass traverses a longer OPL than it would through air. The increase in OPL from the coverslip cannot exceed the depth of field of the objective ($\sim 133 \mu\text{m}$ for experiments in this study). If the shift in OPL is greater than the depth of field enabled by the objective lens, then the image will not appear in focus at the length fixed in the reference arm of the interferometer. However, calculations shown below reveal conditions in which transmitting light through a thin coverglass over the sample will not prevent light interference.

Using Eq. (1), the depth of field (d_{tot}) for an interferometric objective can be calculated. For experiments in this work, the lens had 2.5 \times magnification (M) with numerical aperture (NA) of 0.07. The middle wavelength (λ_o) of illuminating light was $\sim 550 \text{ nm}$ (from a green LED). The smallest lateral resolving distance (e) is 3.8 μm , and the refractive index (n) of the immersion media (air) is 1. Given these parameters, the depth of field is $\sim 133 \mu\text{m}$, which is in the order of the thickness of the cover glass. Since the angle of incidence is small, the OPL through glass can be approximated as the thickness multiplied by the refractive index ($\text{OPL} = T \times n$), and the optical path difference (OPD) is simply the difference between the thickness and the OPL ($\text{OPD} = \text{OPL} - T$). Table 1 shows the thicknesses of various grades of glass coverslips and the corresponding OPD caused by imaging through the glass

$$d_{\text{tot}} = \frac{\lambda_o n}{\text{NA}^2} + \frac{n}{M \times \text{NA}} e. \quad (1)$$

Coverslips up to $\sim 250 \mu\text{m}$ are suitable for transmission imaging with a low-magnification lens because the OPD does not exceed the depth of field. Table 2 shows the decline in depth of field at higher magnification. The narrow depth of field for high-magnification lenses limits the ability to image through glass viewing windows. Even at magnification as low as 5 \times , the depth of field is prohibitively narrow. With higher magnification it would be necessary to compensate for the OPD by inserting a sample of equal thickness in

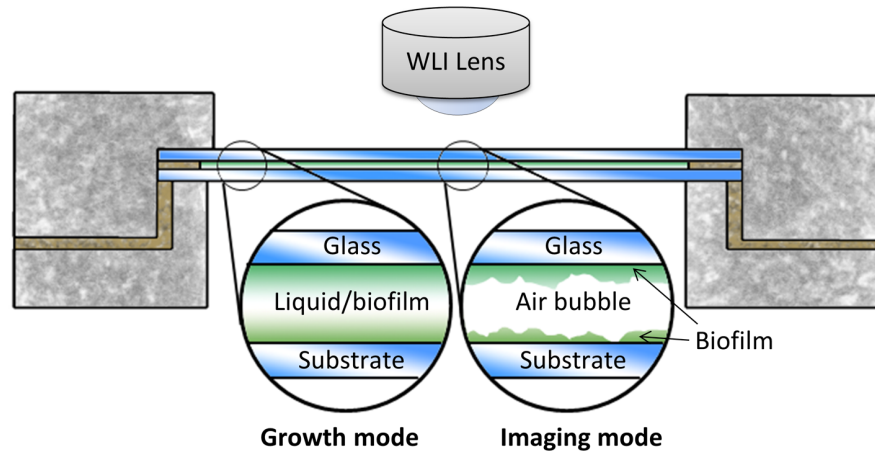


Fig. 4 Cross-sectional view of flow cell shows the thin liquid layer between a glass coverslip and a substrate that forms the growth chamber. Two projected views show the flow cell filled with liquid nutrient broth that supports biofilm growth and with air inserted for imaging. In growth mode, liquid media is pumped through the channel to supply nutrients to bacteria, which form biofilm on all upper and lower surfaces of the flow cell. In imaging mode, an air bubble is introduced into the channel. The air presses against the biofilm, providing a reflective air/water interface that is suitable for imaging. The viewing window is 25-mm wide, and the space for biofilm growth is $\sim 300 \mu\text{m}$.

Table 1 The OPD of several coverslips of varying thickness

Coverslip	Thickness (μm)	OPD (μm) ^a
No. 0	85 to 130	42.5 to 65
No. 1	130 to 160	65 to 80
No. 1.5	160 to 190	80 to 95
No. 2	190 to 230	95 to 115
No. 3	250 to 350	125 to 175

^aCalculated as the difference between OPL and thickness

the reference arm of the interferometer.²⁰ In any case, the spatial resolution of the low-magnification lens is sufficient for observing a biofilm's morphology, and the large field of view is actually an advantage over other imaging modalities. The thickness of the biofilm must also be considered when selecting a viewing window, as the water contained in the biofilm will also contribute to a shift in OPL. For experiments in this work, No. 2 coverslips were used because

Table 2 Depth of field for lenses of different magnification.

Magnification	Depth of field (μm) ^a
2.5	133
5	42
10	6.4
20	3.5
50	1.8

^aCalculated using Eq. (1).

their added thickness reduced the incidence of cracking as a result of pressure induced by the pumping system. Thinner viewing windows would be desirable for imaging thick biofilms but may also require added support because of the tendency to crack under the pressure induced by pumping nutrient broth through the system.

Imaging through a glass coverslip results in multiple sets of interference fringes. Figure 5 shows that interference is seen at the top surface of the glass window and at the bottom surface of the window, which is where it meets biofilm. A final set of fringes with lower intensity is observed at the surface of the biofilm when an air bubble is present. Although the amplitude of this latter fringe packet is much lower than that of the prior two, it is still easily measurable above the noise floor. The refractive index of the glass and the biofilm must be taken into account when calculating the

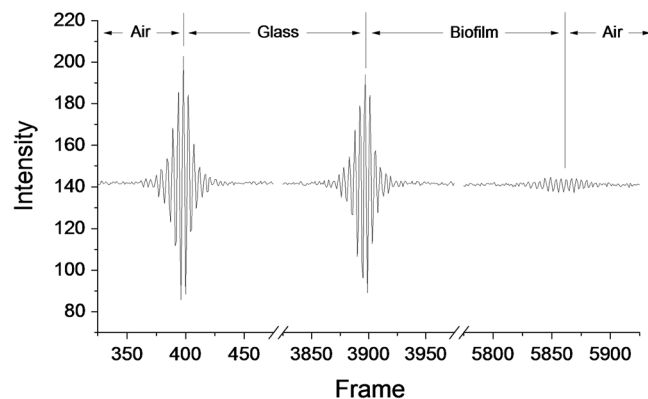


Fig. 5 Imaging through a glass coverslip results in multiple sets of interference fringes. The figure shows an example of multiple interference fringes observed at a single pixel. Interference is observed at the top and bottom of the glass viewing window and from the surface of the biofilm. Light is transmitted through the glass and the biofilm to reach its surface. Each frame on the horizontal scale is a two-dimensional image that is collected during vertical scanning. The physical distance between each surface can be calculated using the group refractive index of each medium (air, glass, and biofilm).

physical distance between each surface. In practice, a vertical range that starts just below the first air/glass interface is selected when collecting data, which results in capture of only the final two sets of interference fringes. Together they can be used to measure thickness and surface roughness of the biofilm. Imaging artifacts can be observed if the biofilm is too thin because the interference fringes overlap and cannot be easily deconvoluted.

3.3 Biofilm Imaging

Figures 6–8 show examples of WLI images of biofilms grown under flow conditions in the flow cell described above. These examples were chosen to demonstrate the strengths and limitations of using WLI to image biofilms. Figure 6 shows the complex heterogeneous structure of a bacterial biofilm on the left side of the image. There are small independent colonies and larger interconnected structures. The right side of the image is smooth, but not because biofilm is absent in this region. The arc that cuts through the center of the image is the leading edge of the air bubble that was inserted into the flow cell. Biofilm is visible and can be imaged interferometrically with the air bubble but cannot be seen without the air bubble.

Figure 7 also has a region in the center of the image with no biofilm. In contrast to Fig. 6, this is not because the region lacks an air bubble. Here, the hydrodynamic effects of flowing liquid media have created a channel where biofilm growth was limited. This image highlights one of the strengths of WLI imaging. The large field of view ensures that a large and salient feature is not overlooked. Imaging with a traditional method with a more limited field of view would require stitched assembly of a large number of images to attain the same level of detail. The biofilm structures seen in Fig. 7 also indicate hydrodynamic influence. In the image, flow of liquid media was from left to right. The biofilm has formed small scalloped features as a result of liquid flow. Figure 8 shows a portion of Fig. 7 in 3-D. The images indicate that the combination of WLI imaging and flow cells could be used to study hydrodynamic effects on biofilms.

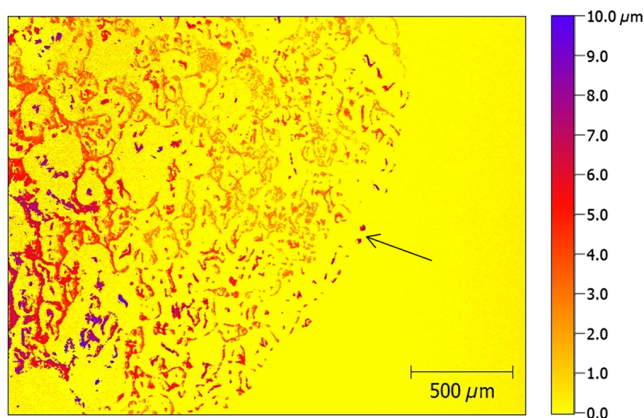


Fig. 6 Example of biofilm image at the edge of a microbubble of air as captured in a flow cell. The left side of the image shows the interconnected nature of a developing biofilm of *P. fluorescens*. Biofilm is not visible at the right of the image because the air bubble was not present under this area. The edge of the bubble is indicated with an arrow. The image is false colored according to the vertical scale at right. The horizontal scale shown by the bar is 500 μm .

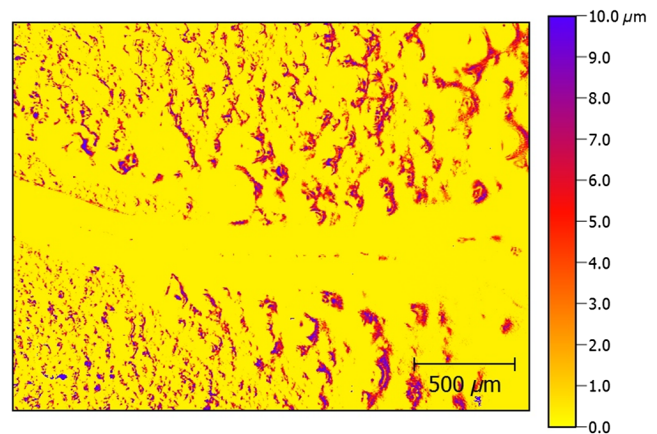


Fig. 7 WLI image shows a flow channel among small scalloped microfeatures of a *P. fluorescens* biofilm. The presence of the channels and the morphology of biofilm features are indicative of growth in flow conditions. Flow of liquid media was from left to right. Features can extend over millimeters or result in small separated microcolonies. The image is false colored according to the vertical scale at right. The horizontal scale shown by the bar is 500 μm .

3.4 Effects of Imaging Method on Biofilm Structure

As described above, WLI is a noncontact and nondestructive imaging method. However, it is clear that the flow cell and air bubble used to create a reflective surface require physical contact with the biofilm and this may impact the structure of the biofilm, especially where bacteria are weakly attached. The interface of a biofilm is known to contain streamers of loosely attached bacteria. These features may be removed or compressed with the insertion of air. In a prior study of the effects of shear flows on biofilms, it was shown that wall shear stress can be calculated if the hydraulic diameter and flow velocity of the system are known.²¹ Hydraulic diameter (D_h) is calculated from the height (H) and width (W) of the flow channel

$$D_h = \frac{4HW}{2(H+W)}. \quad (2)$$

The highest flow velocity encountered in the system can be estimated from the average flow velocity (v_{ave})

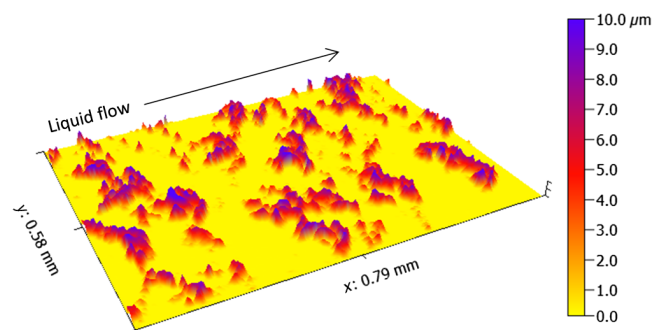


Fig. 8 A section of the image shown in Fig. 7 is shown here in 3-D. WLI produces high-resolution topographical images of biofilm. This image is representative of the heterogeneity encountered in biofilms. There is a wide range of thicknesses. The image is false colored according to the vertical scale at right.

$$v_{\max} = \frac{3}{2} v_{\text{ave}}. \quad (3)$$

Then the wall shear stress (τ_w) can be calculated from the hydraulic diameter, the maximum flow velocity, and the dynamic viscosity of water (η) with the following equation:

$$\tau_w = \frac{4\eta v_{\max}}{D_h}. \quad (4)$$

In this study, the average flow velocity was estimated to be 4.5 mm/s (the bubble filled a 45-mm-long channel in 10 s) with maximum flow velocity of 6.725. The hydraulic diameter was 0.8 mm ($H = 0.5$ mm and $W = 19$ mm). A reference value of 0.001 Pa · s was used for dynamic viscosity of water. Then the shear stress on the biofilm was estimated to be 0.034 Pa. The aforementioned study of shear stress on biofilms²¹ indicates that this shear stress is in line with the shear stress encountered during low-velocity growth phase (0.04 Pa in that study) and at least 1 order of magnitude lower than shear stresses that caused irreversible compression and/or erosion of the biofilm (0.6 to 3.6 Pa). The advantage in the method presented here is that the bubble can be introduced at a very low velocity to minimize impact. Our experiments showed that the bubble did not remove biofilm completely, although further study is needed to study the impact of the imaging process.

In addition to shear stress, the bubble presses down on the biofilm and conforms to its surface. In practice, the conformation of the bubble exerts a normal pressure that is not significantly higher than atmospheric pressure. Nonetheless, it is still higher than the pressure exerted when no bubble is present. Thus, it is likely that the biofilm is compressed when the bubble is present, especially with components with less structural integrity. A comparison of images collected with WLI and a traditional optical technique, such as confocal microscopy, would be useful for confirming this and quantifying the effect.

The results presented in this paper demonstrate that WLI is suitable for biofilm imaging when coupled with an imaging cell with appropriate optical properties. With the flow cell described here, a biofilm can be grown in dynamic flow conditions and can be imaged at regular intervals. Nonetheless, there are several limitations that could be overcome in future research. Multiple measurements have been made in the same location, but more research is needed to establish repeatability of the method. This would also better characterize any adverse effects of placing an air bubble in direct contact with the biofilm. To date, multiple measurements of a biofilm indicate that larger colonies and aggregate structures are persistent; however, lateral resolution of the optical microscope at low magnification is too low to see effects on individual microbes. Finally, while the flow cell described in the paper enables growth of biofilm in dynamic conditions, it is still currently necessary to stop flow for imaging. In future experiments, it may be desirable to explore the benefits and drawbacks of dynamic laser interferometric imaging systems.

4 Conclusions

This paper presents the design of a flow cell that supports growth of bacterial biofilm and is compatible with WLI imaging and describes a WLI biofilm imaging methodology.

An important feature of the flow cell is the viewing window, which is selected to enable light interference without shifting the biofilm's surface out of the field of view of the objective lens. The viewing window enables WLI imaging of biofilm grown in an enclosed and well-controlled environment. The flow cell has influent and effluent channels that support a consistent supply of nutrient broth to a growth chamber where biofilm is cultured. The flow cell is designed to create an interface at the surface of the biofilm that can reflect light back to the imaging objective. Imaging through a glass coverslip results in multiple sets of interference fringes, and data collected during an extended vertical scanning range can resolve each of these interfaces. Biofilm thickness and surface texture can be resolved *in situ* and nondestructively. Example images demonstrate that WLI imaging can be used to observe hydrodynamic effects that are indicative of biofilm growth in flowing liquid. This technique will enable future research on the structure, development, and response of bacterial biofilms in well-controlled growth conditions. Given the unique capabilities, further exploration of bioimaging applications for WLI is warranted.

Acknowledgments

This work was performed at the Pacific Northwest National Laboratories (PNNL), a multiprogram national laboratory operated for the United States Department of Energy by Battelle Memorial Institute under Contract No. DE AC06-76RLO 1830. The work was supported by the Chemical Imaging Initiative and by the Microbiomes in Transition Initiative as part of PNNL's Laboratory Directed Research and Development program. The authors state no conflicts of interest.

References

1. J. W. Costerton et al., "Microbial biofilms," *Annu. Rev. Microbiol.* **49**(1), 711–745 (1995).
2. W. J. Costerton and M. Wilson, "Introducing biofilms," *Biofilms* **1**, 1–4 (2004).
3. L. Hall-Stoodley, J. W. Costerton, and P. Stoodley, "Bacterial biofilms: from the natural environment to infectious diseases," *Nat. Rev. Microbiol.* **2**(2), 95–108 (2004).
4. S. S. Socransky and A. D. Haffajee, "Dental biofilms: difficult therapeutic targets," *Periodontology 2000* **28**(1), 12–55 (2002).
5. M. Elliott et al., "Reductions of *E. coli*, echovirus type 12 and bacteriophages in an intermittently operated household-scale slow sand filter," *Water Res.* **42**(10), 2662–2670 (2008).
6. H.-C. Flemming and J. Wingender, "The biofilm matrix," *Nat. Rev. Microbiol.* **8**(9), 623–633 (2010).
7. J. Xiao et al., "The exopolysaccharide matrix modulates the interaction between 3D architecture and virulence of a mixed-species oral biofilm," *PLoS Pathog.* **8**(4), e1002623 (2012).
8. J. W. Costerton, P. S. Stewart, and E. P. Greenberg, "Bacterial biofilms: a common cause of persistent infections," *Science* **284**(5418), 1318–1322 (1999).
9. A. Beceiro, M. Tomás, and G. Bou, "Antimicrobial resistance and virulence: a successful or deleterious association in the bacterial world?" *Clin. Microbiol. Rev.* **26**(2), 185–230 (2013).
10. G. Wolf, J. G. Crespo, and M. A. M. Reis, "Optical and spectroscopic methods for biofilm examination and monitoring," *Rev. Environ. Sci. Biotechnol.* **1**(3), 227–251 (2002).
11. P. S. Stewart, "Mechanisms of antibiotic resistance in bacterial biofilms," *Int. J. Med. Microbiol.* **292**(2), 107–113 (2002).
12. K. Ross and E. Billing, "The water and solid content of living bacterial spores and vegetative cells as indicated by refractive index measurements," *J. Gen. Microbiol.* **16**(2), 418–425 (1957).
13. M. I. Zibaii et al., "Measuring bacterial growth by refractive index tapered fiber optic biosensor," *J. Photochem. Photobiol. B* **101**(3), 313–320 (2010).
14. J. Reed et al., "High throughput cell nanomechanics with mechanical imaging interferometry," *Nanotechnology* **19**(23), 235101 (2008).
15. J. Reed et al., "Mechanical interferometry of nanoscale motion and local mechanical properties of living zebrafish embryos," *ACS Nano* **3**(8), 2090–2094 (2009).

16. J. Reed et al., "Live cell interferometry reveals cellular dynamism during force propagation," *ACS Nano* **2**(5), 841–846 (2008).
17. C. Larimer et al., "In situ non-destructive measurement of biofilm thickness and topology in an interferometric optical microscope," *J. Biophotonics* **9**(6), 656–666 (2016).
18. S. A. Cruz et al., "Bursting the bubble on bacterial biofilms: a flow cell methodology," *Biofouling* **28**(8), 835–842 (2012).
19. B. Purevdorj, J. Costerton, and P. Stoodley, "Influence of hydrodynamics and cell signaling on the structure and behavior of *Pseudomonas aeruginosa* biofilms," *Appl. Environ. Microbiol.* **68**(9), 4457–4464 (2002).
20. S. Han, "Interferometric testing through transmissive media," *Proc. SPIE* **6293**, 629305 (2006).
21. F. Blauert, H. Horn, and M. Wagner, "Time-resolved biofilm deformation measurements using optical coherence tomography," *Biotechnol. Bioeng.* **112**(9), 1893–1905 (2015).

Curtis Larimer is a materials scientist in the Chemical and Biological Signature Science group at Pacific Northwest National Laboratory (PNNL). He is engaged in basic and applied research at the nexus

of chemistry, materials, and biology. His work has focused on non-destructive chemical and biological imaging.

Michelle Brann was a visiting researcher at PNNL from 2015 to 2016. She is currently pursuing her PhD in chemistry at the University of Chicago.

Jonathan D. Suter is a biomedical engineer in the Applied Optics group at PNNL. He is involved in research aimed at metrology of complex surfaces, including metals, plastics, fabrics, biological tissues, and radiological samples, using both atomic force microscopy and white-light interferometry.

R. Shane Addleman is a senior research scientist at PNNL. His research has focused on analytical methods for chemical, biological, radiological, nuclear, and explosive trace materials. His current work focuses on enhanced trace collection and detection, applied optical and spectroscopic methods, and innovative inorganic and organic separation techniques.